U-series dating of speleothems from the Sierra del Endrinal (Grazalema Mountains, S Spain)

J.M. Alcaraz-Pelegrina [a,*], A. Martínez-Aguirre [b], J. Rodríguez-Vidal [c]

[a] Departamento de Física, Facultad de Ciencias, Universidad de Córdoba, Campus de Rabanales, Ctra de Madrid N-IV-a, km 396, 14071 Córdoba, Spain
[b] Departamento de Física Aplicada I, EUITA, Universidad de Sevilla, Ctra, de Utrera, km 1, 41013 Seville, Spain
[c] Departamento de Geodinámica y Paleontología, Facultad de Ciencias Experimentales, Universidad de Huelva, Campus del Carmen, Avda Tres de Marzo, s/n, 21071 Huelva, Spain

HIGHLIGHTS

- Uranium series dating applied to date karstic mountains in the south of Spain.
- The leachate–leachate method was used to obtain activity ratios in the carbonate fraction.
- The ages obtained range from 34.4 ky to 266 ky.

ABSTRACT

Keywords:

U-series dating
Karst landform
Impure carbonate
Leachate–leachate method

The uranium-series method is applied to date relic flowstone from karstic mountains in the south of Spain. Geomorphological mapping shows three staircased erosion surfaces with a typical karst landform. Exhumed flowstones fill the surficial palaeosinkholes and open fractures. Some of the samples analysed were impure carbonates consequently the leachate–leachate method was used to obtain activity ratios in the carbonate fraction. The ages obtained range from 34.4 ky to 266 ky and are grouped in four periods: 30–50 ky, 90–110 ky, 150 ky and 230–270 ky. All these periods are related to the warm climate oxygen isotope stages 3 and 5. Practically all locations present secular equilibrium in uranium isotopes.

1. Introduction

Uranium series disequilibrium could be applied to study numerous geological, climatic and archaeological problems (Ivanovich and Harmon, 1992). In particular, U/Th dating of carbonates allows us to obtain dates from carbonates as old as 350–500 ky and in the recent decades has been applied to numerous systems around the world (Kaufman et al., 1998; Burns et al., 1998; Zazo et al., 1999; Kelly et al., 2000). It is generally accepted that continental carbonates (speleothems and travertines) are formed in warm Quaternary episodes (Henning et al., 1983; Maire, 1990; Gordon and Smart, 1994). Hence, they are good warm-climate markers in regions such as the Mediterranean, although there are records of substantial accumulations of carbonates in cold episodes (Durán, 1996).

The Iberian Peninsula is very rich in carbonate systems of the Quaternary, and the last few decades have seen much work on them. However, there are few reports on U-series dating in these systems (Bischoff et al., 1988, 1994; Juliá and Bischoff, 1991; Openshaw et al., 1997). In this work, the U–Th age of the samples collected in the Sierra del Endrinal (South of Spain) will be determined, and the problems arising from such analysis in this type of sample will be studied. So, its major aim is methodological.

The Sierra del Endrinal forms part of a larger mountainous group known as the Sierra de Grazalema (Fig. 1); located at the western end of the Betic Cordillera. In this system the karst is markedly developed, both surficially and subterraneously (Delannoy and Díaz del Olmo, 1986). Numerous flowstones can be found in the area. These are thinly laminated deposits formed from groundwaters flowing down cave walls and floors. These were originally formed in the vadose zone of the endokarst some meters below the original surface during a period of predominant carbonatation. Today, after thousands of years of erosion and lowering of the relief, they outcrop at the bare surface at different points in the mountains. The U/Th dating of these exhumed flowstones, and their relation with the various subaereal phases of relief evolution, enable the establishment of an evolutionary chronology of the karstic landscape.

* Corresponding author. Tel.: +34 957212551; fax: +34 957218627.
E-mail address: fa1alpej@uco.es (J.M. Alcaraz-Pelegrina).

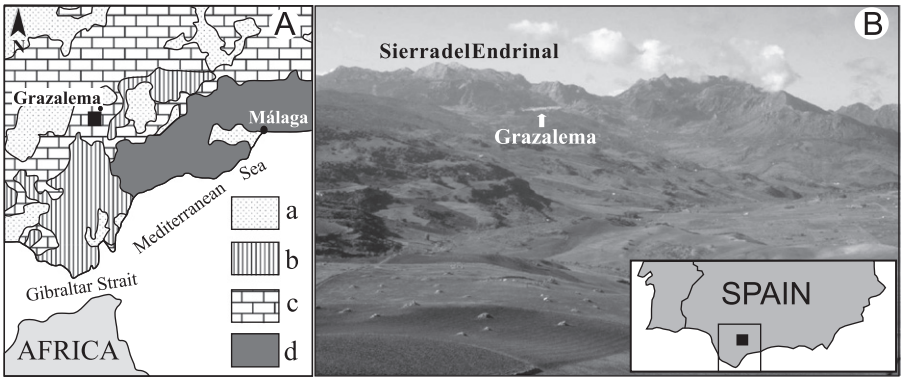

Fig. 1. (A) Geological location of the Sierra del Endrinal. Legend: (a) Neogene and Quaternary formations, (b) Flysch Unit, (c) Subbetic, (d) Alboran Domain. (B) General view of northern Grazalema Mountains and Sierra del Endrinal.

The work therefore started with a geomorphological mapping arranging these forms relatively in time, and then analysing a succession of speleothems by the method of disequilibrium in the uranium series ($^{230}Th/^{234}U$).

The U–Th series is used for dating carbonate deposits because uranium's water-solubility allows its precipitation with calcite. However, thorium is quickly absorbed or precipitated as insoluble hydrolysates when brought into solution. As a result, when calcite is formed, it contains uranium but is thorium-free. The growth of ^{230}Th from its parents enables us to obtain the age of the system (Ivanovich and Harmon, 1992). Unfortunately, most calcite deposits of interest to geology, archaeology, etc. are dirty calcite—the carbonates are mixed with detrital materials that have been deposited with the carbonates. These detrital materials contain uranium and thorium isotopes, and for this reason it is necessary to correct the result obtained from the analyses of carbonates. Because detrital ^{230}Th is always accompanied by ^{232}Th, the presence of detrital materials can be recognised by the presence of ^{232}Th in the thorium spectrum of the samples, and correction for the detrital contribution can be achieved using various correction methods: leachate–residue methods (L/R method) (Ku et al., 1979; Ku and Liang, 1984), the leachate–leachate method (L/L method) (Schwarcz and Latham, 1989), and total sample dissolution method (TSD methods) (Bischoff and Fitzpatrick, 1991; Luo and Ku, 1991). A review of all these methods can be found in Kaufman (1993). All correction methods consider the carbonate sample as a mixture of pure carbonate and detrital material mixed with pure carbonate. Detrital material includes all materials containing uranium and thorium isotopes. L/R methods calculate activity ratios in carbonates from those in leachate and insoluble residue of a sample. There are two L/R methods: correction scheme I (Ku et al., 1979) and correction scheme II (Ku and Liang, 1984). To obtain activities in pure carbonate, the first assumes secular equilibrium in the detrital material and no fractionation between thorium isotopes during dissolution, while correction scheme II assumes no fractionation between uranium and thorium isotopes. In numerous situations, such assumptions are not met, and thus the two methods have limited application. In the L/L method (Schwarcz and Latham, 1989), various leachates of coeval subsamples of a carbonate are needed to obtain activity ratios in pure carbonates from the slopes of the two isochrons described by

$$\left(\frac{^{230}Th}{^{232}Th}\right)_L = \left(\frac{^{230}Th}{^{238}U}\right)_C \left(\frac{^{238}U}{^{232}Th}\right)_L + \frac{r_0}{r_2}\left(\frac{^{230}Th}{^{232}Th}\right)_D - \frac{r_8}{r_2}\left(\frac{^{230}Th}{^{238}U}\right)_C \left(\frac{^{238}U}{^{232}Th}\right)_D \quad (1)$$

$$\left(\frac{^{234}U}{^{232}Th}\right)_L = \left(\frac{^{234}U}{^{238}U}\right)_C \left(\frac{^{238}U}{^{232}Th}\right)_L + \frac{r_4}{r_2}\left(\frac{^{234}U}{^{232}Th}\right)_D - \frac{r_8}{r_2}\left(\frac{^{234}U}{^{238}U}\right)_C \left(\frac{^{238}U}{^{232}Th}\right)_D \quad (2)$$

where the isotope symbol indicates activity of that isotope, and subscripts C, D, and L mean carbonate, detrital material and leachate fraction, respectively. The only assumption of the L/L method is that if fractionation occurs, it must be the same for all samples. Moreover, fractions r_i/r_j must be the same for all samples, where r_i represents the fraction of isotope i[1] in detrital material leachate during dissolution. The TSD method (Bischoff and Fitzpatrick, 1991; Luo and Ku, 1991) totally dissolves the sample, obtaining similar isochrons to those described for the L/L method, with r_i values equal to one. It is more time-consuming as the samples must be dissolved completely, and it can be applied only to inhomogeneous samples in order to obtain different values for the activity ratios to define the isochrons.

Some work (Sharp et al., 2003; Haase-Schramm et al., 2004) includes the U and Th contribution from admixed detritus in carbonate and initial Th in the hydrogenous component, but this approach basically makes two corrections using L/R methods. Of the methods mentioned above, the so-called L/L method seems to give good results, and can be applied to practically all types of impure carbonates (Przybylowicz et al., 1991; Alcaraz-Pelegrina and Martínez-Aguirre, 2005).

2. Materials and methods

The morphology presented by the Sierra del Endrinal consists of mesetas or staircased platforms morphostructural in nature (Fig. 2A). The present work has studied those situated at 1400–1500 m and at 1200 m. These platforms are surrounded by steep slopes having drops of 100–200 m, and are almost subcircular or oval in shape, although with some embayments caused by the capture of dolinised areas by fluvial erosion.

The surfaces of these mesetas are intensely karstified. Their relief is of gentle slopes and rounded hillocks, from an ancient karst cover that has become exhumed. Over this earlier relief lies a surface created from bare karren, related with recent, functional erosion–corrosion, an uncovered, active karst. This morphogenetic alternation has probably been repeated with some frequency throughout the Quaternary, due to climatic changes.

[1] $i=8$ for ^{238}U, $i=4$ for ^{234}U, $i=0$ for ^{230}Th and $i=2$ for ^{232}Th.

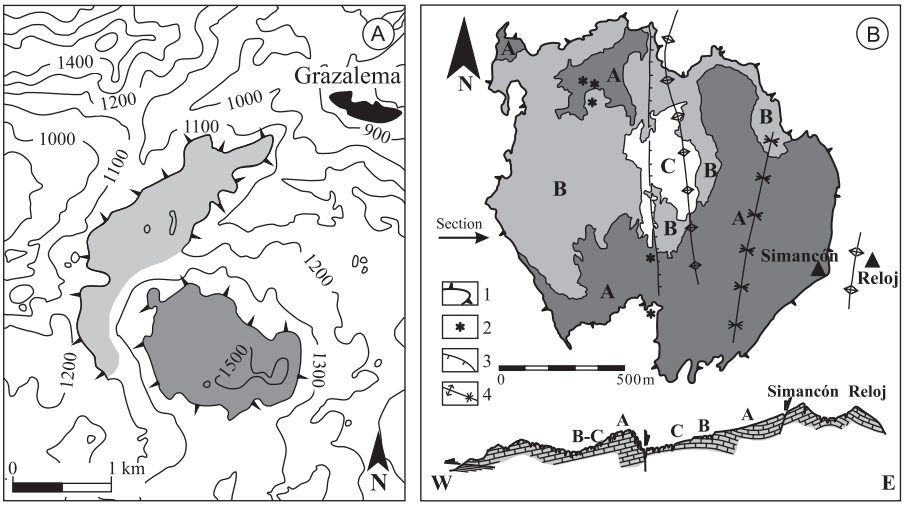

Fig. 2. (A) Geographical situation of both karst platforms. (B) Geomorphological sketch of the upper karstic platform (1400 m) and its geological cross section. Key: (1) upper platform boundary, (2) speleothem sample site, (3) fault, (4) fold (anticline at left, sincline at right), A, B, C, erosion surfaces.

Table 1
U–Th analytical results for samples of 1400 m platform. Number in parentheses indicates nitric acid concentration used during sample dissolution. (F) indicates fired samples prior to dissolution. Errors are $1-\sigma$.

Sample	^{238}U (ppm)	$\frac{^{234}U}{^{238}U}$	$\frac{^{230}Th}{^{234}U}$	$\frac{^{230}Th}{^{232}Th}$	ρ_{0242}	ρ_{0282}	ρ_{8242}	Age (ka)
1400 m platform								
Sima GR-85: 1434 m.a.s.l								
Gz-1A	0.076 ± 0.002	0.973 ± 0.029	0.598 ± 0.031	36 ± 5	–	–	–	99.5 ± 8.5
Gz-1B	0.076 ± 0.002	1.030 ± 0.025	0.553 ± 0.026	77 ± 11	–	–	–	86.9 ± 6.3
Mean value		1.001 ± 0.045	0.575 ± 0.026					92.8 ± 6.7
Sima GR-65: 1423 m.a.s.l.								
Gz-2A	0.050 ± 0.002	1.062 ± 0.041	0.985 ± 0.069	12.6 ± 1.3	0.832	0.856	0.934	> 350
Gz-2B	0.057 ± 0.002	0.942 ± 0.034	0.934 ± 0.065	9.4 ± 0.9	0.721	0.773	0.956	> 350
Gz-2C	0.052 ± 0.002	0.996 ± 0.037	0.829 ± 0.064	13.7 ± 1.8	0.949	0.949	0.990	192 ± 43
Gz-2D	0.054 ± 0.002	1.017 ± 0.035	0.862 ± 0.055	10.8 ± 0.9	0.747	0.401	0.563	212 ± 44
Sima GR-168: 1428 m.a.s.l.								
Gz-3A	0.042 ± 0.002	1.004 ± 0.039	0.926 ± 0.060	61 ± 15	–	–	–	280 ± 87
Gz-3B	0.027 ± 0.002	1.009 ± 0.042	0.938 ± 0.064	109 ± 37	–	–	–	297 ± 108
Mean Value		1.007 ± 0.042	0.932 ± 0.064					289^{+163}_{-71}
Sima KL-42: 1410 m.a.s.l.								
GZ-4A	0.061 ± 0.003	1.014 ± 0.049	0.873 ± 0.076	9.67 ± 1.01	0.748	0.736	0.921	221^{+93}_{-50}
Gz-4B	0.055 ± 0.002	1.052 ± 0.039	0.931 ± 0.070	9.33 ± 0.86	0.773	0.726	0.885	271^{+170}_{-65}
Gz-4C	0.061 ± 0.003	1.001 ± 0.031	0.968 ± 0.082	7.7 ± 0.7	0.736	0.736	0.999	> 350
Gz-4D	0.056 ± 0.003	1.065 ± 0.039	0.905 ± 0.069	11 ± 1	0.714	0.776	0.999	240^{+96}_{-51}
N-S Fault: 1444 m.a.s.l.								
Gz-5A (2)(F)	0.119 ± 0.004	1.044 ± 0.022	0.867 ± 0.046	5.93 ± 0.26	0.380	0.363	0.999	212 ± 35
Gz-5B (4)(F)	0.128 ± 0.005	0.974 ± 0.022	0.954 ± 0.049	5.84 ± 0.21	0.311	0.291	0.962	> 350
Gz-5C (7)(F)	0.126 ± 0.005	0.959 ± 0.024	1.025 ± 0.054	4.89 ± 0.14	0.204	0.207	0.998	> 350
Gz-5D (2)	0.110 ± 0.005	0.994 ± 0.034	0.464 ± 0.027	10.9 ± 0.8	0.568	0.568	0.994	68 ± 6
Gz-5E (4)	0.111 ± 0.005	1.014 ± 0.036	0.614 ± 0.034	8.30 ± 0.41	0.451	0.451	0.917	103 ± 10
Gz-5F (6)	0.113 ± 0.004	1.038 ± 0.028	0.624 ± 0.033	7.48 ± 0.34	0.385	0.385	0.974	105 ± 10
N-S fault: 1465 m.a.s.l.								
Gz-6A	0.115 ± 0.003	0.995 ± 0.018	0.460 ± 0.015	ND	–	–	–	66.8 ± 3.1
Sima GR-85(-50 m): 1372 m.a.s.l.								
Gz-7A	0.083 ± 0.002	1.018 ± 0.030	0.845 ± 0.045	68 ± 11	–	–	–	200 ± 30
Gz-7B	0.076 ± 0.002	1.043 ± 0.027	0.932 ± 0.048	114 ± 29	–	–	–	275 ± 70
Mean value		1.029 ± 0.082	0.887 ± 0.046					231^{+51}_{-35}

Exhumed speleothem deposits are numerous in the two platforms studied. These calcitic flowstones are usually situated subvertically or inclined, occupying ancient open fractures, cracks, cavities, or pit walls, and they grow outwards from the surface of the rock; sometimes with accretion of calcitic layers from both walls of the fissure, other times having a single direction of growth. Thus, the relative antiquity of each layer in a speleothem can be determined. A total of 10 speleothem samples were collected for this work: seven in the 1400 m platform and four in the 1200 m platform, as indicated in Tables 1 and 2 and in Fig. 2B. All samples were collected at the surface, except Gz-7, which was a horizontal flowstone at the

Table 2
U–Th analytical results for samples of 1200 m platform. Number in parentheses indicates nitric acid concentration used during sample dissolution. (F) indicates fired samples prior to dissolution. Errors are $1-\sigma$.

Sample	^{238}U (ppm)	$\frac{^{234}U}{^{238}U}$	$\frac{^{230}Th}{^{234}U}$	$\frac{^{230}Th}{^{232}Th}$	ρ_{0242}	ρ_{0282}	ρ_{8242}	Age (ka)
1200 m platform								
Sima GR-15: 1226 m.a.s.l.								
Gz-8	0.068 ± 0.001	0.985 ± 0.018	0.291 ± 0.010	22 ± 3	–	–	–	37.4 ± 1.6
25 m SW of Sima GR-15: 1245 m.a.s.l.								
Gz-9A (7)(F)	0.116 ± 0.005	0.994 ± 0.038	0.973 ± 0.061	2.05 ± 0.06	0.624	0.615	0.907	>350
Gz-9B (2)(F)	0.155 ± 0.006	1.013 ± 0.032	0.949 ± 0.060	2.13 ± 0.07	0.574	0.574	0.989	>350
Gz-9C (7)	0.137 ± 0.005	1.085 ± 0.040	0.642 ± 0.039	2.87 ± 0.12	0.542	0.534	0.994	109 ± 11
Gz-9D (2)	0.128 ± 0.005	1.096 ± 0.038	0.497 ± 0.029	3.24 ± 0.15	0.540	0.540	0.999	74 ± 6
Sima GR-30: 1230 m.a.s.l.								
Gz-10	0.133 ± 0.001	0.979 ± 0.013	0.290 ± 0.011	33 ± 5	–	–	–	37.2 ± 1.7

bottom of a sinkhole (-50 m). Each sample is the oldest one for each location, being collected from the bottom of each speleothem site. All samples show no evidence of recrystallisation.

Some of the samples (Gz-2, Gz-4, Gz-5, and Gz-9) presented detrital material mixed with the carbonate; these were treated as impure carbonates, and the L/L method was used to obtain the activity ratios in pure carbonate needed for age determination.

Pure carbonates were dissolved using 2 M nitric acid. For impure carbonates, various approaches can be used to obtain the 4–6 coeval, carbonate–detrital mixture, required for each isochron age determination of a sample according to the L/L method (Alcaraz-Pelegrina, 2003; Przybylowicz et al., 1991; Kelly et al., 2000). We used here the two approaches summarised below:

- Dissolution of subsamples containing varied carbonate–detrital material proportions with the same acid. Thus, differences in activity concentrations are due to differences in carbonate–detrital ratio in the different subsamples. Impure carbonates Gz-2 and Gz-4 were prepared in this way and were dissolved using concentrated nitric acid.
- Crushing and homogenising the sample. Various subsamples are dissolved with different nitric acid concentrations. Here, differences in activity concentrations are due to the distinct nitric acid concentrations. Some of the samples were also fired at 900 °C for 3 h prior to dissolution in order to have a wider range of values. Impure carbonates Gz-5 and Gz-9 were prepared in this way.

In the cases of both pure and impure carbonates, the solution is separated by filtration as soon as possible after dissolution to avoid thorium reabsorption onto the detrital residue. During dissolution a known amount of ^{232}U and ^{229}Th is added for yield calculations. ^{229}Th is used as thorium spike because impure carbonates have a certain ^{228}Th content. Some subsamples are fired at 900 °C prior to dissolution in order to obtain a wide range of values for the isochrons (Bischoff and Fitzpatrick, 1991). Procedures for the isolation and purification of uranium and thorium are detailed in Alcaraz-Pelegrina (2003). In leachates, an iron carrier ($FeCl_3$) is added. Iron hydroxides are precipitated at pH 9 with concentrated ammonia. The precipitate is dissolved in 8 M HNO_3 and a solvent extraction method with tributylphosphate (TBP) is used to backextract uranium and thorium from dissolution into the organic phase. After separation, 20 ml of xylene is mixed with the TBP phase and 1.5 M HCl (as the inorganic phase) is used to extract thorium from the organic phase. Finally, uranium is back-extracted from the organic phase with distilled water. The uranium fraction is ready for electroplating, while the thorium fraction needs further purification as some uranium traces are also back-extracted with the thorium. For this reason, we used an anion-exchange resin for thorium purification. A few ml of iron carrier is added to it, and iron hydroxides are precipitated. This precipitate is dissolved in 1:1 volume of 8 M HCl and concentrated HCl. The solution is added to an anion-exchange resin (AG 1X8 Dowex) column (4 cm long) conditioned with 8 M HCl. Uranium traces and iron remain on the column and thorium is collected in a beaker. Iron carrier is added to the solution and iron hydroxides are again precipitated. The precipitate is dissolved in nitric acid. A second column with the same resin, conditioned with 7 M nitric acid, is used to purify the thorium fraction. Iron and other impurities pass through the resin, while thorium remains. The thorium is finally collected by adding 2 M HCl to the column. This solution is ready for electroplating. Some 0.3 M $NaSO_4$ is added to the final solutions, which are evaporated to dryness. The electrodeposition of uranium and thorium is performed for 1 h at 1.2 A. One minute before switching off the current, 1 ml of NH_3 is added.

The planchets are measured by alpha spectrometry (García-Toraño, 2006). The alpha spectrometer system used was equipped with PIPS detectors and showed good stability over 3–7 days of counting time generally required for each planchet. Moderate-to-high recovery yields and well-resolved spectra provided analytically reliable results.

3. Results and discussion

Tables 1 and 2 show uranium concentration, activity ratios, and nominal ages for samples from the 1400 m platform and 1200 m platform, respectively. For impure carbonates, we include error correlations used in Rosholt diagrams. These error correlations are calculated according to Ludwig and Titterington (1994), as are the ages of impure carbonates that are obtained using UISO (Ludwig, 1993) and ISOPLOT (Ludwig, 1991) programs. These ages are summarised in Table 3 which also include initial $^{234}U/^{238}U$. Figs. 3 and 4 show Rosholt diagrams for impure carbonates as 2-D versions for illustration purposes only, because the activity ratios $^{230}Th/^{234}U$ and $^{234}U/^{238}U$ in the carbonate fraction are derived by a 3-D fit to the data. ^{238}U activities range from 0.5 to 1.9 mBq/g, sufficient to be measured easily by α-spectrometry. Moderate-to-high recovery yields and well resolved alpha spectra provided analytically reliable results.

As can be seen in Tables 1 and 2, samples Gz-1, Gz-3, Gz-6, Gz-7, Gz-8, and Gz-10 were free of detrital ^{230}Th contamination, or it can be ignored. Thus, various replicates were prepared, except for Gz-6, Gz-8 and Gz-10, and mean values used for age determination. In these samples, uranium concentration ranges from 0.3 (Gz-3) to 1.65 mBq/g (Gz-10), and all samples present secular equilibrium between uranium isotopes. Samples Gz-2, Gz-4, Gz-5, and Gz-9 had detrital ^{230}Th contamination, indicated by activity ratios $^{230}Th/^{232}Th$ lower than 15 in all cases. For some

Table 3
Activity ratios and ages obtained using UISO program. MSWD means mean square of weighted deviates of the data from the regression lines and P.o.f. is the probability of fit as reported by UISO programs. Errors are $1-\sigma$.

Sample	$\frac{^{230}Th}{^{234}U}$	$\frac{^{234}U}{^{238}U}$	Age (ky)	MSWD	P.o.f.	Initial $\left(\frac{^{234}U}{^{238}U}\right)$
Gz-2	0.632 ± 0.065	1.057 ± 0.050	107 ± 9	0	1	1.077 ± 0.068
Gz-4	0.745 ± 0.172	1.133 ± 0.023	142 ± 69	1.68	0.152	1.198 ± 0.052
Gz-5	0.311 ± 0.021	0.995 ± 0.002	40.6 ± 3.3	0	1	0.994 ± 0.002
Gz-9	0.273 ± 0.028	1.152 ± 0.007	34.4 ± 4.0	0.477	0.753	1.161 ± 0.012

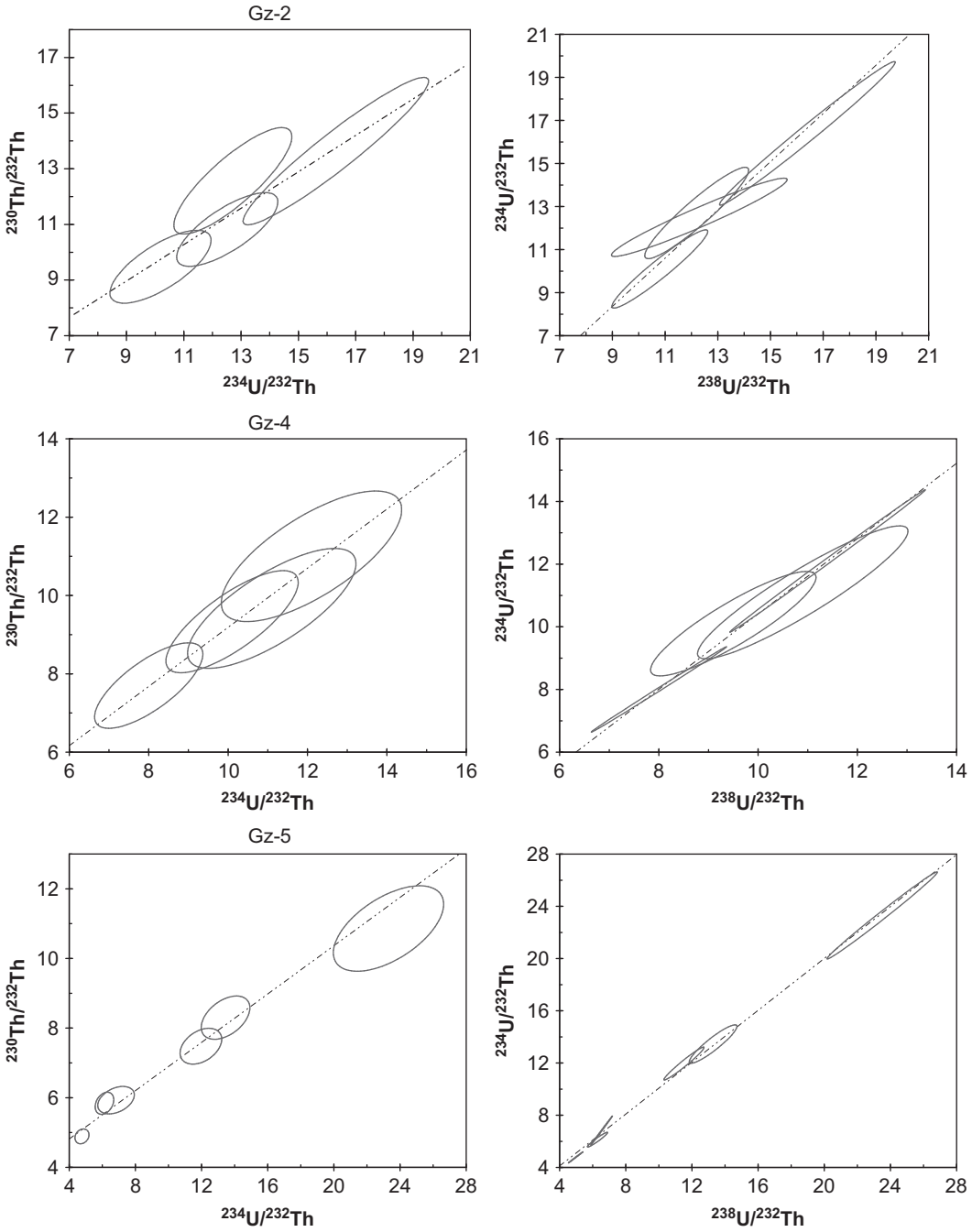

Fig. 3. Rosholt diagrams (2-D version) for 1400 m platform samples. Lines drawn are for illustration purposes only because the activity ratios in carbonate fraction and ages are based on a 3-D isochron fit.

subsamples, recorded ages exceeded 350 ky due to the detrital contribution. Because of this detrital contribution the ages obtained without correction were higher than corrected ages.

As mentioned above, two approaches were used to obtain 4–6 subsamples for the L/L method in order to correct this contamination. Subsamples for Gz-2 and Gz-4 were all dissolved using

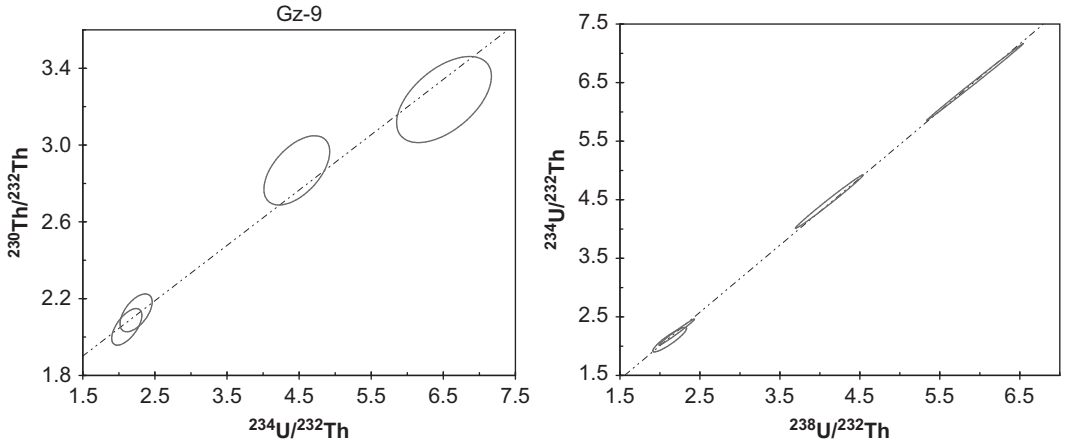

Fig. 4. Rosholt diagrams (2-D version) for 1200 m platform samples. Lines drawn are for illustration purposes only because the activity ratios in carbonate fraction and ages are based on a 3-D fit to the data.

concentrated nitric acid; thus differences in activities are due to different carbonate–detrital ratio in distinct subsamples. Tables 1 and 2 show that these differences are not so high. However, they allow us to define Rosholt diagrams as can be seen in Figs. 3 and 4. For Gz-2 sample, the 3-D fit of data with UISO program gives a value with an acceptable error (around 10%) whereas for Gz-4 sample the age error is nearly 50%.

On the other hand, subsamples for Gz-5 and Gz-9 were homogenised and dissolved using different nitric acid concentrations. As a consequence, we obtained Rosholt diagrams with a wider range of values than those for samples Gz-2 and Gz-4. Moreover, subsamples fired prior to dissolution presented higher activity concentration than did unfired samples, allowing us to define Rosholt diagrams better. This agrees with other results, as in Bischoff and Fitzpatrick (1991), indicating that firing facilitates isotope extraction. This approach to prepare impure carbonates (homogenisation, dissolution) yields better isochron plots. Moreover, firing certain subsamples gives a wider range of activity ratio values for such isochron plots.

Error correlations ρ_{0242} and ρ_{0282} are higher in Gz-2 and Gz-4 samples than in all the others because ^{232}Th activity errors are higher than those of other uranium and thorium isotopes in these two samples. From samples Gz-5, and Gz-9, the two thorium isotope activities have a similar error, giving lower error correlation values. Generally, error correlation ρ_{8242} is close to unity, because uranium activities have error values lower than those of ^{232}Th activity.

Table 4 displays the samples taken, with their ages, limits of error, and altitudinal location. Ages from the 1400 m platform range from 40.6 ± 3.3 ky for Gz-5 to 289^{+163}_{-71} ky for Gz-3 and can be grouped in four periods: 40 ky (Gz-5); 90–110 ky (Gz-1, Gz-2, and Gz-6); 150 ky (Gz-4), and 230–290 ky (Gz-3 and Gz-7). All samples present secular equilibrium between uranium isotopes, except for Gz-4 (1.198 ± 0.052). Ages for the 1200 m platform are younger that those of the 1400 m platform, ranging from 34.4 ± 4.0 ky for Gz-9 to 37.4 ± 1.6 ky for Gz-8. As in the 1400 m platform, all samples present initial $^{234}U/^{238}U$ equal to unity, except for the youngest, Gz-9, which has excess ^{234}U with respect to ^{238}U: 1.161 ± 0.012.

In some samples, as Gz-3, ages have high uncertainties primarily due to the uranium isotopes being in secular equilibrium and the sample age is in the limit of alpha spectrometry resolution.

The ages obtained indicate that most of the samples were formed during the Upper Pleistocene (warm isotope stages 3 and 5), and a minority in the Middle Pleistocene (warm isotope stage 7) with slight deviations towards the cold stages (6 and 8). Thus, there seems to be a good correlation between the genesis of the speleothems and the warm episodes of the last 250 ky.

Table 4
Ages and initial $^{234}U/^{238}U$ for Endrinal Mountains samples.

Sample	Altitude (m.a.s.l.)	Age (ky)	$\left(\frac{^{234}U}{^{238}U}\right)_o$
1400 m Platform			
Gz-1	1434	92.8 ± 6.7	1.001 ± 0.058
Gz-2	1423	107 ± 9	1.077 ± 0.068
Gz-3	1428	289^{+163}_{-71}	1.006 ± 0.072
Gz-4	1410	142 ± 69	1.198 ± 0.052
Gz-5	1444	40.6 ± 3.3	0.994 ± 0.022
Gz-6	1465	67.8 ± 3.1	0.994 ± 0.021
Gz-7	1372	231^{+51}_{-35}	1.059 ± 0.156
1200 m Platform			
Gz-8	1226	37.4 ± 1.6	0.983 ± 0.020
Gz-9	1245	34.4 ± 4.0	1.161 ± 0.012
Gz-10	1230	37.2 ± 1.7	0.977 ± 0.014

In contrast, most of the speleothems from the platform of 1400 m (where the oldest samples were collected) were formed in oxygen isotope stage (OIS) 5, whereas most of the samples taken on the platform of 1200 m were formed in OIS 3. Accordingly, there is a direct relationship between altitude and the age of the speleothems. That is, the earliest phases of carbonatation are better represented at greater altitude, while the most recent are found at the lower altitude. This could indicate that the zones with a more active chemical morphogenesis descend over time, and that there has been a selective conforming of the karstic relief.

The relationship of the different ages on the two platforms also seems to indicate a parallelism and a general joint evolution of both of them.

Similar ages have been obtained by other authors in the Grazalema Mountains region: Delannoy and Díaz del Olmo (1986) and Durán (1996) in the Sierra de Libar, and Delannoy (1992) in the Sierra de las Nieves, all in the province of Málaga (South of Spain).

4. Conclusions

The chronological analysis of the speleothems collected at the surface and at depth in the Sierra del Endrinal has contributed

sufficient data to establish the general lines of the morphoclimatic evolution of a middle-mountain Mediterranean karst with predominantly erosional characteristics.

The analysis of the sampled speleothems shows that for impure carbonates, taking various cogenetic samples after crushing and homogenising the sample, plus firing some of them prior to dissolution, gives better results in generating the isochron date in the L/L method.

The ages obtained range from 34.4 ky (Gz-10) to 266 ky (Gz-3), with ages from the 1200 m platform younger that those from the 1400 m platform. These ages group in four periods: 30–50 ky (Gz-5, Gz-8, Gz-9, and Gz-10) 90–110 ky (Gz-1, Gz-2 and Gz-6), 150 ky (Gz-4) and 230-270 ky (Gz-3, and Gz-7). All these periods are related to warm climate. Except for Gz-9, with initial $^{234}U/^{238}U$ equal to 1.161 ± 0.012, and Gz-4, with 1.198 ± 0.052, all the samples have secular equilibrium in uranium isotopes.

Acknowledgements

We thank the GEOS Caving Group (Seville, Spain) for the field work assistance.

References

Alcaraz-Pelegrina, J., 2003. Aplicación de los desequilibrios en las series naturales a la datación de sistemas carbonatados del sur de España. Ph.D. Thesis, Universidad de Sevilla, Sevilla, España.

Alcaraz-Pelegrina, J., Martínez-Aguirre, A., 2005. Isotopic fractionation during leaching of impure carbonates and their effect on uranium series dating. Quat. Sci. Rev. 24, 2584–2593.

Bischoff, J., Fitzpatrick, J., 1991. U-series dating of impure carbonates: an isochron technique using total-sample dissolution. Geochim. Cosmochim. Acta 55, 543–554.

Bischoff, J., Juliá, R., Mora, R., 1988. Uranium-series dating of the Mousterian occupation at Abric Romani, Spain. Nature 332, 68–70.

Bischoff, J., Ludwig, K., García, J., Carbonell, E., Vaquero, M., Stafford Jr., T., Jull, A., 1994. Dating of the basal aurignacian sandwich at Abric Romaní (Catalunya, Spain) by radiocarbon and uranium-series. J. Archaeol. Sci. 21, 541–551.

Burns, S., Matter, A., Frank, N., Maugini, A., 1998. Speleothem-based paleoclimate record from northern Oman. Geology 26, 499–502.

Delannoy, J., 1992. Les apports de la karstologie dans la définition morphogénique d'un massif montagnard méditerraneén (exemple de la Sierra de las Nieves, Andalousie, Espagne). In: Karst et evolutiones climatiques. Hommage á J. Nicod. Presses Universitaires, Bordeaux., pp. 153–175.

Delannoy, J., Díaz del Olmo, F., 1986. La Serranía de Grazalema (Málaga-Cádiz). Karstologia Mémories 1, 54–70.

Durán, J., 1996. Los sistemas kársticos de la provincia de Málaga y su evolución: Contribución al conocimiento paleoclimático del Cuaternario en el Mediterráneo occidental. Ph.D. Thesis, Universidad Complutense de Madrid, Madrid, España.

García-Toraño, E., 2006. Current status of alpha-particle spectrometry. Appl. Radiat. Isot. 64, 1273–1280.

Gordon, D., Smart, P., 1994. Comments on speleothems, travertines and paleoclimates by G.J. Henning, E. Grün, and K. Brunnacker. Quat. Res. 22, 144–147.

Haase-Schramm, A., Goldstein, S., Stein, M., 2004. U–Th dating of Lake Lisan (late Pleistocene Dead Sea) aragonite and implications for glacial East Mediterranean climate change. Geochim. Cosmochim. Acta 68, 985–1005.

Henning, G., Grün, R., Brunnacker, K., 1983. Speleothems, travertines and paleoclimates. Quat. Res. 20, 1–29.

Ivanovich, M., Harmon, S. (Eds.), 1992. Uranium-series Disequilibrium. Applications to Earth, Marine, Environmental and Sciences, 2nd ed. Oxford University Press.

Juliá, R., Bischoff, J., 1991. Radiometric dating of quaternary deposits and the hominid mandible of Lake Banyolas, Spain. J. Archaeol. Sci. 18, 707–722.

Kaufman, A., 1993. An evaluation of several methods for determining $^{230}Th/U$ ages of impure carbonates. Geochim. Cosmochim. Acta 57, 2303–2317.

Kaufman, A., Wasserburg, G., Porcelli, D., Bar-Matthews, M., Ayalon, A., Halicz, L., 1998. U–Th isotope systematics from the Soreq cave, Israel and climatic correlations. Earth Planet. Sci. Lett. 156, 141–155.

Kelly, M., Black, S., Rowan, J., 2000. A calcrete-based U/Th chronology for landform evolution in the Sorbas basin, southeast Spain. Quat. Sci. Rev. 19, 995–1010.

Ku, T., Bull, W., Freeman, S., Knauss, K., 1979. $^{230}Th–^{234}U$ dating of pedogenic carbonates in gravelly desert soils of Vidal Valley, southeastern California. Geol. Soc. Am. Bull. 90, 1063–1073.

Ku, T., Liang, Z., 1984. The dating of impure carbonates with decay-series isotopes. Nucl. Instrum. Methods Phys. Res. 223, 563–571.

Ludwig, K., 1991. ISOPLOT. A plotting and regression program for radiogenic-isotope data. USGS Open-File Report 445.

Ludwig, K., 1993. UISO. A program for calculation of $^{230}Th–^{234}U–^{238}U$ isochrons. USGS Open-File Report 531.

Ludwig, K., Titterington, D., 1994. Calculation of $^{230}Th/U$ isochrons, ages and errors. Geochim. Cosmochim. Acta 58, 5031–5042.

Luo, S., Ku, T., 1991. U-series isochron dating: a generalized method employing total-sample dissolution. Geochim. Cosmochim. Acta 55, 555–564.

Maire, R., 1990. La haoute montagne calcaire. In: Karstologia Mémories, vol. 3, p. 17.

Openshaw, S., Latham, A., Shaw, J., 1997. Speleothem palaeosecular variation record from China: their contribution to the coverage of Holocene palaeosecular variation data in East Asia. J. Geomag. Geoelect. 49, 485–505.

Przybylowicz, W., Schwarcz, H., Latham, A., 1991. Dirty calcites. 2. Uranium-series dating of artificial calcite–detritus mixtures. Chem. Geol. (Isotope Geoscience Section) 86, 161–178.

Schwarcz, H., Latham, A., 1989. Dirty calcites. 1. Uranium-series dating of contaminated calcite using leachates alone. Chem. Geol. (Isotope Geoscience Section) 80, 35–43.

Sharp, W., Ludwig, K., Chadwick, O., Amundson, R., Glaser, L., 2003. Dating fluvial terraces by $^{230}Th/U$ on pedoginic carbonate, Wind River basin, Wyoming. Quat. Res. 59, 139–150.

Zazo, C., Silva, P., Goy, J., Hillaire-Marcel, C., Ghaleb, B., Lario, J., Bardají, T., González, A., 1999. Coastal uplift in continental collision plate boundaries: data from the last interglacial marine terraces of the gibraltar strait area (South Spain). Tectonophysics 301, 95–109.